



Thermal Barrier Coatings for Gas-Turbine Engine Applications

Nitin P. Padture,^{1*} Maurice Gell,¹ Eric H. Jordan²

Hundreds of different types of coatings are used to protect a variety of structural engineering materials from corrosion, wear, and erosion, and to provide lubrication and thermal insulation. Of all these, thermal barrier coatings (TBCs) have the most complex structure and must operate in the most demanding high-temperature environment of aircraft and industrial gas-turbine engines. TBCs, which comprise metal and ceramic multilayers, insulate turbine and combustor engine components from the hot gas stream, and improve the durability and energy efficiency of these engines. Improvements in TBCs will require a better understanding of the complex changes in their structure and properties that occur under operating conditions that lead to their failure. The structure, properties, and failure mechanisms of TBCs are herein reviewed, together with a discussion of current limitations and future opportunities.

The great difference in the thermo-mechanical properties of metals and ceramics would seem to preclude their use in composite structures subjected to huge changes in temperature and thermal stresses. Nonetheless, thermal barrier coatings (TBCs) made of low-thermal conductivity ceramics are now being used to provide thermal insulation to metallic components from the hot gas stream in gas-turbine engines used for aircraft propulsion, power generation, and marine propulsion (1–4). The use of TBCs (100 to 500 μm in thickness), along with internal cooling of the underlying superalloy component, provide major reductions in the surface temperature (100° to 300°C) of the superalloy. This has enabled modern gas-turbine engines to operate at gas temperatures well above the melting temperature of the superalloy (~1300°C), thereby improving engine efficiency and performance. Alternatively, at somewhat lower operating temperatures, TBCs help reduce metal temperature, making engine components more durable. TBCs are also being used, to some extent, in diesel engines, where higher operating temperatures translate into increased fuel economy and cleaner exhaust (3).

The structure of a thermal barrier-coated component consists of four layers—two ceramic and two metallic—with each layer having markedly different physical, thermal, and mechanical properties, making it inherently more complex than the individual components that are all metallic or all

ceramic. The thermal barrier-coated component must withstand the most extreme temperature, temperature cycling, and stress conditions, and it is expected to last thousands of take-offs and landings in commercial jet engines and up to 30,000 hours of operation in industrial gas-turbine engines. The combination of the multimaterial nature of the TBC structure and the demanding operating conditions make TBCs more complex than any other coating system.

Although the number and the severity of TBC applications have dramatically increased in the past decade, premature spallation-failure of TBCs during service, which can expose the bare metal to dangerously hot gases, is still an overriding concern. The mechanisms by which TBCs fail are varied, and the factors that are responsible are numerous, the most important among which are (i) the thermal-expansion mismatch stresses; (ii) the oxidation of the metal; and (iii) the continuously changing compositions, microstructures, interfacial morphologies, and properties of the TBC system.

The concern of premature failure has slowed the use of TBCs, and even where used, the full temperature advantage, and hence energy efficiency and operating lifetime, offered by TBCs has not been realized. TBCs are an example of a material system where technology has largely preceded scientific understanding. It is recognized that a basic understanding of TBC materials and failure must be gained if TBCs are to achieve their full potential of being designed and applied to last the lifetime of the component. This has been the focus of intense research activity in the past decade. The complexity and diversity of

TBC structures and the severity of operating conditions make this a challenging task. TBC is perhaps the only system where a complex interplay occurs of all of the following phenomena: diffusion, oxidation, phase transformation, elastic deformation, plastic deformation, creep deformation, thermal expansion, thermal conduction, radiation, fracture, fatigue, and sintering. However, this also presents a unique opportunity to distill the rich and varied behavior of TBCs, and to analyze it in terms of fundamental principles governing materials phenomena for gaining generic understanding.

Here, we present a description of TBC material systems presently in use, a summary of current understanding of materials and failure issues in TBCs, and the future outlook, highlighting challenges and opportunities in TBC research and development.

Anatomy of a TBC

The four layers in the current TBC system (Fig. 1) are made of different materials with specific properties and functions. These layers are (i) the substrate, (ii) the bond-coat, (iii) the thermally grown oxide (TGO), and (iv) the ceramic top-coat.

Substrate. The nickel- or cobalt-based structural superalloy is the substrate material, which is air-cooled from the inside or through internal hollow channels, thus establishing a temperature gradient across the component wall. The superalloy component is investment-cast in single-crystal or polycrystalline forms, and it contains as many as 5 to 12 additional elements that are added for the enhancement of specific properties such as high-temperature strength, ductility, oxidation resistance, hot-corrosion resistance, and castability (5). At the high temperature of operation in gas-turbine engines, diffusion of elements of high relative concentration can occur between the superalloy substrate and the bond-coat. These diffusing elements can occasionally be found in the TGO and the top-coat as well (6). This interdiffusion can have a profound influence on the spallation failure of the TBC, making it necessary to treat thermal barrier-coated superalloys as an engineering system whose properties change with time and cycles during service.

Bond-coat and thermally grown oxide

¹Department of Metallurgy and Materials Engineering,
²Department of Mechanical Engineering, Institute of Materials Science, University of Connecticut, Storrs, CT 06269–3136, USA.

*To whom correspondence should be addressed. E-mail: nitin.padture@uconn.edu

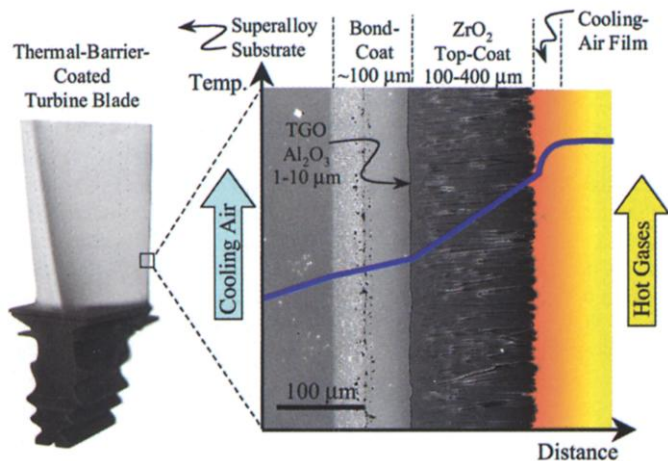


Fig. 1. Cross-sectional scanning electron micrograph (SEM) of an electron-beam physical-vapor deposited (EB-PVD) TBC, superimposed onto a schematic diagram showing the temperature reduction provided by the TBC. The turbine blade contains internal hollow channels for air-cooling, whereas the outside hot-section surface is thermal barrier-coated, setting up a temperature gradient across the TBC.

(TGO). The bond-coat is an oxidation-resistant metallic layer, 75 to 150 μm in thickness, and it essentially dictates the spallation failure of the TBC. The bond-coat is typically made of a NiCrAlY or NiCoCrAlY alloy and is deposited by using the plasma-spray or the electron-beam physical-vapor deposition methods. Other types of bond-coats are made of aluminides of Ni and Pt and are deposited by electroplating in conjunction with diffusion-aluminizing or chemical-vapor deposition. In a minority of cases, the bond-coat consists of more than one layer, having a different chemical/phase composition.

At peak operating conditions the bond-coat temperature in gas-turbine engines typically exceeds 700°C, resulting in bond-coat oxidation and the inevitable formation of a third layer—the thermally grown oxide (TGO; 1 to 10 μm in thickness)—between the bond-coat and the ceramic top-coat (7). The interconnected porosity that always exists in the top-coat allows easy ingress of oxygen from the engine environment to the bond-coat. Moreover, even if the top-coat were fully dense, the extremely high ionic diffusivity of oxygen in the ZrO₂-based ceramic top-coat renders it “oxygen transparent” (8).

Although the formation of the TGO is inevitable, the ideal bond-coat is engineered to ensure that the TGO forms as $\alpha\text{-Al}_2\text{O}_3$ and that its growth is slow, uniform, and defect-free. Such a TGO has a very low oxygen ionic diffusivity and provides an excellent diffusion barrier, retarding further bond-coat oxidation (9). Generally, the inward diffusion of oxygen through the TGO controls further growth of TGO into the bond-coat, but in some cases TGO growth is controlled by outward diffusion of Al, leading to the formation of the new TGO at the TGO/top-coat interface or at the $\alpha\text{-Al}_2\text{O}_3$ grain boundaries within the TGO (7, 9, 10). Finally, the bond-

coat, whereas elements that promote adhesion (Si, Hf) are added in small quantities (14, 15).

Ceramic top-coat. This layer provides the thermal insulation and is typically made of Y₂O₃-stabilized ZrO₂ (YSZ) (3). YSZ possesses a suite of desirable properties that make it the material of choice for the top-coat. It has one of the lowest thermal conductivities at elevated temperature of all ceramics [$\sim 2.3 \text{ W}\cdot\text{m}^{-1}\cdot\text{K}^{-1}$ at 1000°C for a fully dense material (16)] because of its high concentration of point defects (oxygen vacancies and substitutional solute atoms), which scatter heat-conducting phonons (lattice waves) (17). YSZ also has a high thermal-expansion coefficient ($\sim 11 \times 10^{-6} \text{ }^\circ\text{C}^{-1}$), which helps alleviate stresses arising from the thermal-expansion mismatch between the ceramic top-coat and the underlying metal ($\sim 14 \times 10^{-6} \text{ }^\circ\text{C}^{-1}$). To further alleviate these stresses, microstructural features such as cracks and porosity are deliberately engineered into the top-coat, making it highly compliant (elastic modulus $\sim 50 \text{ GPa}$) and “strain tolerant.” YSZ has a relatively low density ($\sim 6.4 \text{ Mg}\cdot\text{m}^{-3}$), which is important for parasitic-weight considerations in rotating engine components. It also has a hardness of $\sim 14 \text{ GPa}$, which makes it resistant to erosion and foreign-body impact. YSZ is resistant to ambient and hot corrosion.

coat composition is designed to obtain a highly adherent TGO (11). It is known that the segregation of S at the bond-coat/TGO interface reduces the TGO adhesion dramatically (12). To mitigate this adverse effect of S, either the S content in the bond-coat is maintained below 1 part per million or S-“gettering” reactive elements (Y, Zr) are added (13). Other elements that degrade the bond-coat/TGO adhesion (Ti, Ta) are also kept below acceptable levels in the

Finally, YSZ has a high melting point ($\sim 2700^\circ\text{C}$), making it suitable for high-temperature applications.

Although ZrO₂ can be stabilized by a host of different oxides (MgO, CeO₂, Sc₂O₃, In₂O₃, CaO), Y₂O₃-stabilized ZrO₂ (YSZ) has been empirically found to be most suitable for TBC applications (3). YSZ exists as three different polymorphs—monoclinic, tetragonal, and cubic—depending on the composition and the temperature (18). The addition of 7 to 8 weight % (~ 4 to 4.5 mol%) Y₂O₃ stabilizes the *t'*-phase, the most desirable phase for TBC applications (3). This is a variation of the tetragonal phase, but unlike its low Y₂O₃-containing (~ 3 mol%) counterpart, the *t'* phase does not undergo a martensitic transformation and is, therefore, more stable (18).

Although there are various methods for depositing ceramic coatings on metal substrates, the two most important methods used for TBC top-coat deposition are (i) air-plasma-spray (APS) deposition and (ii) electron-beam physical-vapor deposition (EB-PVD). These two methods produce characteristic microstructures with certain desirable attributes that are discussed below.

Air-plasma-sprayed TBCs. Based on many years of process development, APS TBCs have the following favorable microstructural characteristics (Fig. 2) (3): (i) “splat” grain morphology (1 to 5 μm thick, 200 to 400 μm diameter) with inter-“splat” boundaries and cracks parallel to the metal/ceramic interface for low thermal conductivity and (ii) 15 to 25 vol% porosity for both low elastic modulus (high “strain tolerance”) and low thermal conductivity. However, the undulating nature of the metal/ceramic interface, which is required for better interlocking adhesion, produces out-of-plane stresses responsible for in-service failure of APS TBCs as described below. A typical APS top-coat is 300 μm thick, but in some industrial gas-turbine engines applications it can reach 600 μm in thickness. The orientation of the cracks and pores normal to the heat flow

reduces the thermal conductivity of the top-coat from $\sim 2.3 \text{ W}\cdot\text{m}^{-1}\cdot\text{K}^{-1}$ for a fully dense material to a more typical 0.8 to 1.7 $\text{W}\cdot\text{m}^{-1}\cdot\text{K}^{-1}$ (19).

Versatility and low production cost make APS TBCs attractive commercially. However, because of the proliferation of microstructural defects parallel to the interface and the roughness of the interface, APS TBCs

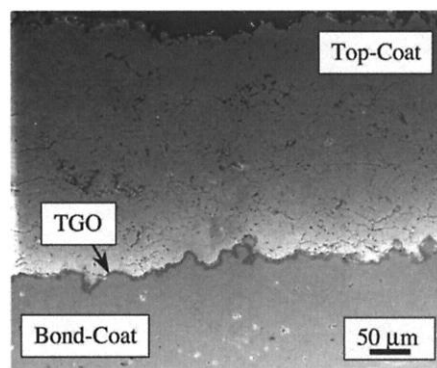


Fig. 2. Cross-sectional SEM of an air-plasma-sprayed (APS) TBC that has been subjected to 120 thermal cycles. Each 60-min cycle constitutes 50 min at 1120°C followed by 10 min of forced-air cooling to ambient temperature.

generally have shorter thermal-cycling lives than EB-PVD TBCs. This makes APS TBC suitable only for less exacting applications in aircraft engines, such as combustors, fuel vaporizers, after-burner flame holders, and stator vanes. APS TBCs have served extremely well in industrial gas-turbine engines, including “bucket” (blade) and “nozzle” (vane) applications, because of lower operating temperatures, reduced temperature gradients, and fewer thermal cycles.

Electron-beam physical-vapor deposited TBCs. In contrast to the APS case, here the bond-coat surface can be smooth before deposition. Typically, EB-PVD top-coats ($\sim 125\ \mu\text{m}$ thick) have the following microstructural features (Fig. 1) (3, 20): (i) thin region of polycrystalline YSZ with equiaxed grains (size 0.5 to $1\ \mu\text{m}$) at and near the metal/ceramic interface; (ii) columnar YSZ grains (2 to $10\ \mu\text{m}$ diameter) growing out of the equiaxed-grain region to the top-coat surface; (iii) nanometer-scale porosity within the columnar grains; and (iv) channels separating the columnar grains, normal to the metal/ceramic interface.

The disconnected columns impart “strain tolerance” to the TBC because they can separate at high temperatures, accommodating thermal-expansion mismatch stresses (20). The porosity and the cracks help reduce the thermal conductivity [~ 1.5 to $2\ \text{W}\cdot\text{m}^{-1}\cdot\text{K}^{-1}$ (21)], but to a lesser extent than APS TBCs, because the channels are parallel to the direction of heat flow. EB-PVD TBCs are more durable, but expensive, relative to APS TBCs, and are used primarily in the most severe applications, such as turbine blades and vanes in aircraft engines.

Damage Accumulation and Failure

During engine operation, several interrelated time- and cycle-dependent phenomena take place within the TBC system that ultimately result in the TBC failure by spallation of the top-coat. This wide variation of conditions is one of the reasons why TBC failure mechanisms are not completely understood. To further complicate matters, a large number of different TBC systems are used, each one intended for a particular component and engine. For example, power-generation engines for utilities operate for long periods of time with only a few shut-down cycles. In contrast, aircraft engines operate at full capacity (takeoff and landing) for only a few minutes, resulting in shorter but more numerous thermal cycles. Despite the enormous

complexities, generic understanding of TBC failure mechanisms is beginning to emerge, and is discussed below.

The growth of the TGO during engine operation is the most important phenomenon responsible for the spallation failure of TBCs. TGO growth sometimes results in a constrained volume expansion that leads to compressive “growth” stresses [$<1\ \text{GPa}$ (22)] that persist at all temperatures. Upon cooling, the thermal-expansion mismatch between the TGO and the bond-coat leads to very high “thermal” compressive residual stresses in the TGO that reach a maximum at ambient

bond-coat (27). Such roughening, often termed “ratcheting,” requires thermal cycling and does not occur during isothermal exposures. It also requires an initial surface-geometry imperfection of some minimum dimension and the progressive lengthening of the TGO either due to TGO cracking or due to in-plane growth during oxidation (28, 29). For a nominally flat bond-coat/TGO interface (EB-PVD TBC), this roughening manifests in the form of TGO penetration into the bond-coat (30, 31). In an already undulated interface, the undulation amplitude is amplified (APS TBC) (4).

All of these geometrical factors result in out-of-plane stresses normal to the metal/ceramic interface, the severity of which increases with thermal cycling. These stresses, in combination with the interfacial imperfections, are primarily responsible for TBC failure.

Damage initiation and progression in the form of microcracks can occur in many different ways in TBCs, depending on the particular TBC, the portion of spallation life already consumed, and the thermal cycling environment. The coalescence of these cracks results in the ultimate spallation failure of the TBC. The detailed failure mechanisms in the two classes of TBCs (APS and EB-PVD) are different and are discussed separately below.

Air-plasma-sprayed TBC. There are at least four primary failure mechanisms in APS TBCs that are driven by the out-of-plane stresses, shown schematically in Fig. 3A (32–34). The stresses at the bond-coat/TGO interface are tensile at the undulation crests and compressive at the troughs (35). As the TGO thickens, the tensile stress increases, which causes cracking at the bond-coat/TGO interface at crests (mechanism I in Fig. 3, A and B) (36).

The thermal-expansion mismatch between the top-coat and the metal (bond-coat/superalloy) puts the top-coat in overall compression at room temperature. However, these stresses are an order of magnitude lower than the residual stresses in the TGO, primarily because the porous and cracked top-coat is much more compliant relative to the TGO, and it has a relatively lower thermal expansion-coefficient mismatch with the bond-coat. Once again, because of the highly undulating nature of the metal/ceramic interface, out-of-plane stresses result in the vicinity of the TGO/top-coat interface: tension at the crests and compression at the troughs (37). The tension causes fracture along the TGO/top-coat interface at the crests (mechanism II in Fig. 3, A and B) and cracking

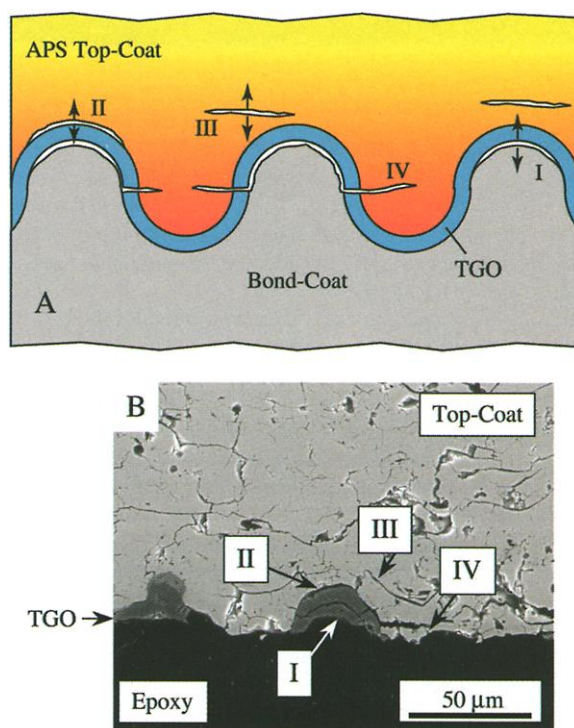


Fig. 3. (A) Schematic diagram showing the four different cracking mechanisms in APS TBC. (B) Cross-sectional SEM of a failed APS TBC (240 cycles) mounted in epoxy (bond-coated substrate not shown) showing the various cracking mechanisms illustrated in (A).

temperature [2 to 6 GPa (23, 24)]. The strain energy in the TGO scales linearly with the TGO thickness and quadratically with the TGO stress, and drives fracture.

The formation and growth of the $\alpha\text{-Al}_2\text{O}_3$ TGO results in the depletion of Al in the bond-coat. The Al depletion, if severe, results in the formation of other oxides, such as Ni- and Co-containing spinels, $\text{Y}_3\text{Al}_5\text{O}_{12}$, and Y_2O_3 (25, 26). The formation of these phases compromises the structural integrity of the TGO and accelerates localized oxidation by providing fast oxygen-diffusion paths.

During thermal cycling, progressive roughening of the bond-coat/TGO/top-coat interfaces occurs due to cyclic creep of the

within the highly brittle top-coat in the vicinity of the crests (mechanism III in Fig. 3, A and C) (33, 34).

As the TGO thickens, it constitutes a good fraction of the bond-coat asperity. Thus, the thermal stresses are locally dominated by the thermal-expansion mismatch between the bond-coat/TGO "composite" asperity, rather than just the bond-coat, and the top-coat. Beyond a certain TGO thickness, the thermal-expansion coefficient of the bond-coat/TGO composite becomes lower than that of both the top-coat and the bond-coat, which reverses the nature of the stresses in the top-coat undulation troughs from compression to tension (34, 38). This reversal causes cracking within the top-coat in the "valleys" between the crests (mechanism IV in Fig. 3, A and B) (34).

Electron-beam physical-vapor TBC. Because the top-coat in EB-PVD TBCs is more "strain tolerant" than that in APS TBCs, the various cracking events in this system occur at the bond-coat/TGO or the TGO/top-coat interfaces. There are three main types of failure mechanisms in this system, two of which are schematically shown in Fig. 4A. Mechanism I, separation of the bond-coat/TGO interface, is the same as that described in the APS TBC case (mechanism I in Fig. 3). The crests in the case of EB-PVD are "ridges" present on the bond-coat surface before top-coat deposition (Fig. 4B) (39). Mechanism II in Fig. 4A is separation of the TGO/top-coat interface and penetration of the TGO into the bond-coat resulting from one or more of the following mechanisms: (i) progressive TGO roughening caused by bond-coat cyclic creep (Fig. 4, B and C) (30, 31); (ii) accelerated growth of embedded oxides due to localized TGO cracking (26, 27, 40); and (iii) cavity formation in the bond-coat (27). For EB-PVD TBCs with relatively flat and defect-free interfaces, the compression in the TGO causes large-scale buckling, as shown in Fig. 4D (39, 41).

In both APS and EB-PVD TBCs, interfacial fracture is assisted by any degradation of the interfacial toughness by fatigue and segregation of undesirable elements to the interface, especially sulfur (13). Sintering within the top-coat at operating temperatures, which results in the partial healing of the cracks and a reduction in porosity, also accelerates TBC failure by making the top-coat less "strain tolerant" (42, 43). In addition, sintering increases the thermal conductivity of the top-

coat (19), resulting in a higher metal surface temperature and the attendant enhancement of bond-coat oxidation and creep.

Life prediction of TBC. Because of the high cost of tooling in the manufacture of gas-turbine engines, there is a great incentive to predict the life of competing designs for turbine parts, rather than identifying superior designs through building and testing. An integral part of the evaluation of the merits of different designs prior to developing hardware is calculating TBC life for previous operating histories. Accordingly, a variety of life-prediction methods have been developed for engineering purposes (44–47). Given the number of potential failure mechanisms, the most accurate

four layers of the TBC; (iii) quantitative models for some processes, especially oxidation behavior in complex multicomponent alloys; and (iv) exact conditions under which one mechanism of failure is replaced by another. Progress in understanding the failure mechanisms has to be based not only on physical experiments but also on increasingly realistic finite element models of local failure modes (29, 40, 48, 49). The state-of-the-art is characterized by rapid improvement of the understanding and modeling of specific failure mechanisms mostly by academic researchers, whereas industry continues to use semiempirical models.

In developing semiempirical models, the two primary goals are (i) to include the correct variables and (ii) to incorporate them in functional forms that provide the best probability of extrapolating current engine experience to future designs where temperatures and other factors may be different. This type of thinking is illustrated by a representative, industrially developed life model that has been published (46). In that model, the primary damage variables chosen are the TGO thickness and mechanical strain range in the TBC. TGO thickness is the most appropriate variable, because it is a measure of stored strain energy and is implicated in most of the damage mechanisms. The use of mechanical strain range captures the idea that larger strain excursions associated with larger temperature excursions are increasingly damaging. Semiempirical models such as this must be calibrated against data to determine a number of empirical parameters. The calibrated version of this model has been successful in predicting failure for the conditions and materials for which it was developed. The ultimate research goal, with respect to life prediction, is to reach a state of knowledge that allows mechanism-based methods to be used in engineering practice. In the interim, improvement in the understanding of operative mechanisms allows for more insightful choices of variables, properties, and functional forms in engineering models.

Future Outlook

Improved materials will continue to play a major role in meeting the gas-turbine industry's requirements for improved durability and energy efficiency. Because the

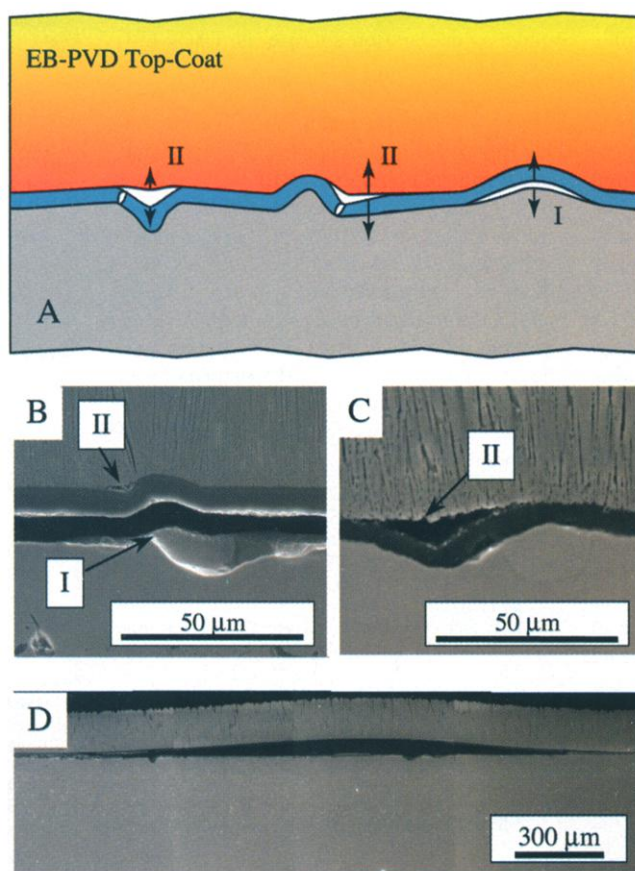


Fig. 4. (A) Schematic diagram showing two of the three different cracking mechanisms in EB-PVD TBC. Cross-sectional SEMs showing (B) mechanisms I and II (1917 cycles), (C) mechanism II (376 cycles), and (D) large-scale buckling (1830 cycles) where bond-coat surface imperfections were eliminated before top-coat deposition.

TBC life-prediction system would be the one for which the failure mechanisms are known for a specific TBC under its relevant engine operating conditions. At present, such life prediction is not practical because of the lack of knowledge, in some cases, of (i) the operative mechanism; (ii) physical and mechanical properties data as a function of temperature and strain rate for the

implementation of alternate high-temperature structural materials such as ceramics, ceramic composites, intermetallics, and refractory metal alloys is still in the developmental stages, the near-term focus will be on TBCs with improved durability and performance. Major improvements in both durability and performance should be achievable by using approaches that are based on the recent understanding of TBC failure mechanisms, and are summarized below.

The durability of current YSZ-based TBCs can be substantially increased with improvements in bond-coat composition and processing. We have seen that the key to durability is the retention of strong bonding between the TGO and the bond-coat. In order to accomplish this, it is necessary (i) to create and maintain a strong initial bond and (ii) to reduce the stresses and accumulated strain energy that promotes cracking at the bond-coat/TGO interface. To create a strong initial bond, it is important that the bond-coat composition and the heat treatment be chosen such that α -Al₂O₃, and not some other transient oxide, is the initial oxide layer that forms on the bond coat, and that all bond-coat surface defects and roughness be eliminated. To maintain a strong bond, the diffusion of deleterious elements such as S, Ti, and Ta from the superalloy substrate or the bond-coat to the interface must be prevented during elevated-temperature service exposure. To that end, considerable progress has been made in reducing sulfur content in alloys (13). To reduce the out-of-plane tensile stress across the interface and the strain energy contained in the TGO, it is desirable to have a flat interface, and to have a creep-resistant bond-coat that reduces further interface roughening during cyclic engine operation in both EB-PVD and APS TBCs. A fourfold improvement in TBC durability has been achieved by reducing the interfacial roughness alone (Fig. 4D) (39). It is also desirable to have a bond-coat composition that reduces the growth rate (thickening) of the TGO and promotes adherence of a thicker TGO.

In APS TBCs, in addition to the cracking that occurs at the bond-coat/TGO interface at bond-coat asperities, there is spallation at the top-coat splat boundaries. Toughening or eliminating these splat boundaries will increase APS TBC durability. This has been achieved by using an innovative plasma-spray process (50). Segmented top-coats with periodic cracks normal to the metal/ceramic interface are desirable for increasing the "strain tolerance" in APS TBCs. A TBC with this feature has been implemented commercially (51). Suppression of sintering within the top-coats (in both EB-PVD and APS TBCs) at operating temperatures is also desirable for maintaining high "strain tolerance" (43).

There is great motivation for developing ceramic top-coats with reduced high-temperature thermal conductivities (43, 52–54). Reduced thermal conductivity will help (i) improve TBC durability by reducing the metal temperature and retarding the thermally activated processes responsible for failure and/or (ii) improve engine efficiency by allowing it to operate at higher temperatures. To reduce thermal conductivity at elevated temperatures, it is necessary to reduce phonon conduction and radiative heat transfer. Phonon conduction can be reduced by choosing new ceramics that contain high concentrations of point defects, such as oxygen vacancies and solute atoms with a high atomic-weight contrast relative to the host (17). Rare-earth zirconates are examples of such ceramics now under consideration for use as TBCs (53, 54). Radiation may be reduced by using suitable reflective coatings. Strategic placement of oriented cracks and pores within the top-coat and suppression of sintering at operating temperatures will also reduce both phonon conduction and radiative heat transfer (55, 56). Although the search for suitable new TBC ceramics continues, success will ultimately come from a fuller appreciation of all of the favorable characteristics that have made YSZ such a successful TBC to date, and the incorporation of these characteristics in a ceramic with lower conductivity and higher use temperature.

References and Notes

- R. A. Miller, *Surf. Coat. Technol.* **30**, 1 (1987).
- S. M. Meier, D. K. Gupta, K. D. Sheffler, *J. Metals* **43**, 50 (1991).
- R. L. Jones, in *Metallurgical and Ceramic Coatings*, K. H. Stern, Ed. (Chapman and Hall, London, 1996), p. 194.
- A. G. Evans, D. R. Mumm, J. W. Hutchinson, G. H. Meier, F. S. Pettit, *Prog. Mater. Sci.* **46**, 505 (2001).
- M. Gell, D. N. Duhl, D. K. Gupta, K. D. Sheffler, *J. Metals* **39**, 11 (1987).
- U. Kaden, C. Leyens, M. Peters, W. A. Kaysser, in *Elevated Temperature Coatings: Science and Technology*, J. M. Hampikian, N. B. Dhotre, Eds. (The Minerals, Metals, Materials Society, Warrendale, OH, 1999), vol. 3, p. 27.
- F. H. Stott, G. C. Wood, *Mater. Sci. Eng.* **A87**, 267 (1987).
- A. C. Fox, T. W. Clyne, in *Proc. 15th Int. Thermal Spray Conf.*, 25 to 29 May 1998, C. Coddet, Ed. (ASM International, Metals Park, OH, 1998), p. 1589.
- P. Kofstad, *High Temperature Corrosion* (Elsevier Applied Science, New York, 1988).
- M. J. Stiger, N. M. Yanar, M. G. Topping, F. S. Pettit, G. H. Meier, *Z. Metallkd.* **90**, 1069 (1999).
- W. J. Brindley, R. A. Miller, *Surf. Coat. Technol.* **43/44**, 446 (1990).
- J. G. Smeggil, *Mater. Sci. Eng.* **A87**, 261 (1987).
- J. L. Smialek, D. T. Jayne, J. C. Schaffer, W. H. Murphy, *Thin Solid Films* **253**, 285 (1994).
- T. E. Strangman, S. J. Vonk, *U.S. Patent No.* 4,743,514 (1988).
- B. A. Pint, J. A. Haynes, K. L. Moore, I. G. Wright, C. Leyens, in *Superalloys 2000*, K. A. Green, T. M. Pollock, R. D. Kissinger, Eds. (The Minerals, Metals, Materials Society, Warrendale, PA, 2001), p. 629.
- D. P. H. Hasselman, et al., *Am. Ceram. Soc. Bull.* **66**, 799 (1987).
- P. G. Klemens, in *Thermal Conductivity*, K. E. Wills, R. B. Dinwiddie, R. S. Graves, Eds. (Technomic, Lancaster, PA, 1993), vol. 23, p. 209.
- E. C. Subbarao, in *Science and Technology of Zirconia*, A. H. Heuer, L. W. Hobbs, Eds. (American Ceramic Society, Columbus, OH, 1984), vol. 3, p. 1.
- H. E. Eaton, J. R. Linsey, R. B. Dinwiddie, in *Thermal Conductivity 22*, T. W. Tong, Ed. (Technomic, Lancaster, PA, 1994), p. 289.
- T. E. Strangman, *Thin Solid Films* **127**, 93 (1985).
- M. Peters, K. Fritscher, G. Staniek, W. A. Kaysser, U. Schultz, *Materialwissen. Werkstofftech.* **28**, 357 (1997).
- E. Schumann, C. Sarioglu, J. R. Blachere, F. S. Pettit, G. H. Meier, *Oxid. Metals* **53**, 259 (2000).
- D. M. Lipkin, D. R. Clarke, *Oxid. Metals* **45**, 267 (1996).
- K. W. Schlichting et al., *Mater. Sci. Eng.* **A291**, 68 (2000).
- E. Y. Lee, R. R. Biederman, R. D. Sisson, *Mater. Sci. Eng.* **A121**, 467 (1989).
- D. R. Mumm, A. G. Evans, *Acta Mater.* **48**, 1815 (2000).
- M. Gell et al., *Surf. Coat. Technol.* **120-121**, 53 (1999).
- J. M. Ambrico, M. R. Begley, E. H. Jordan, *Acta Mater.* **49**, 1577 (2001).
- A. M. Karlsson, A. G. Evans, *Acta Mater.* **49**, 1793 (2001).
- A. G. Evans, M. Y. He, J. W. Hutchinson, *Prog. Mater. Sci.* **46**, 249 (2001).
- Y. H. Sohn, J. H. Kim, E. H. Jordan, M. Gell, *Surf. Coat. Technol.* **146**, 70 (2001).
- R. A. Miller, C. E. Lowell, *Thin Solid Films* **95**, 265 (1982).
- A. Rabieli, A. G. Evans, *Acta Mater.* **48**, 3963 (2000).
- K. W. Schlichting, N. P. Padture, E. H. Jordan, M. Gell, *Mater. Sci. Eng. A*, in preparation.
- X. Y. Gong, D. R. Clarke, *Oxid. Metals* **50**, 355 (1998).
- D. R. Clarke, W. Pompe, *Acta Mater.* **47**, 1749 (1999).
- C. H. Hsueh, P. F. Becher, E. R. Fuller, S. A. Langer, W. C. Carter, *Mater. Sci. Forum* **308-311**, 442 (1999).
- C. H. Hsueh, E. R. Fuller, *Scripta Mater.* **42**, 781 (2000).
- K. Vaidyanathan, M. Gell, E. H. Jordan, *Surf. Coat. Technol.* **133-134**, 28 (2000).
- J. Cheng, E. H. Jordan, B. Barber, M. Gell, *Acta Mater.* **46**, 5839 (1998).
- A. G. Evans, J. W. Hutchinson, *Int. J. Solids Struct.* **20**, 455 (1984).
- D. Zhu, R. A. Miller, *Surf. Coat. Technol.* **108-109**, 114 (1998).
- C. Leyens et al., *Z. Metallkd.* **92**, 762 (2001).
- R. A. Miller, *J. Eng. Gas Turbines Power* **109**, 448 (1987).
- T. A. Cruse, S. E. Stewart, M. Ortiz, *J. Eng. Gas Turbines Power* **110**, 610 (1988).
- S. M. Meier, D. M. Nissley, K. D. Sheffler, S. Bose, *J. Eng. Gas Turbines Power* **114**, 521 (1992).
- P. K. Wright, *Mater. Sci. Eng.* **A245**, 191 (1998).
- G. C. Chang, W. A. Phucharoen, R. A. Miller, *Surf. Coat. Technol.* **30**, 29 (1987).
- A. M. Fregborg, B. L. Ferguson, W. J. Brindley, G. J. Petrus, *Mater. Sci. Eng.* **A245**, 182 (1998).
- N. P. Padture et al., *Acta Mater.* **49**, 2251 (2001).
- D. M. Gray, Y.-C. Lau, C. A. Johnson, M. P. Borom, W. A. Nelson, *U.S. Patent No.* 6,180,184 (2001).
- N. P. Padture, M. Gell, P. G. Klemens, *U.S. Patent No.* 6,015,630 (2000).
- M. J. Maloney, *U.S. Patent No.* 6,117,560 (2000).
- R. Subramanian, *U.S. Patent No.* 6,258,467 (2001).
- J.-M. Dorvaux et al., in *Proceedings of the 85th Meeting Advisory Group Aerospace Research and Development, Structures and Materials Panel*, 15 to 16 October 1997 (NATO, Neuilly-sur-Seine, France, 1998), p. 13.
- K. W. Schlichting, N. P. Padture, P. G. Klemens, *J. Mater. Sci.* **36**, 3003 (2001).
- We thank K. Schlichting for providing figures 2 and 3 and K. Vaidyanathan for providing figures 1 and 4. Funding for this work was provided by the U.S. Department of Energy and the Office of Naval Research.